Proceedings of the 28th IEEE
EMBS Annual International Conference
New York City, USA, Aug 30-Sept 3, 2006

New Deformable Registration Technique Using Scale Space and Curve Evolution Theory and A Finite Element Based Validation Framework

Rachid Fahmi, Alaa Aly, Ayman Elbaz, Student Members, IEEE, and Aly A. Farag, Senior Member, IEEE.

Abstract— **In this paper, we present a novel and accurate approach for nonrigid registration. New feature descriptors are built as voxel signatures using scale space theory. These descriptors are used to capture the global motion of the imaged object. Local deformations are modelled through an evolution process of equi-spaced closed curves/surfaces (iso-contours/surfaces) which are generated using fast marching level sets and are matched using the built feature descriptors. The performance of the proposed approach is validated using the finite element method. Both 2D and 3D tissue deformations cases are simulated, and the registration accuracy is quantified by co-registering the deformed images with the original ones and comparing the recovered mesh point displacements with the simulated ones. The evaluation results show the potential of the proposed approach in handling local deformation better than some conventional approaches.**

I. INTRODUCTION

Registration is a major component in many medical image analysis applications. Registration techniques can be categorized into two main families: feature-based and intensity-based techniques. The feature-based methods rely on extracting and matching salient anatomical structures from images (edges, contours, line intersections, corners, etc.). The intensity-based methods are used directly to match image intensities without any attempt to detect distinctive objects. This paper is not intended to give a comprehensive survey on image registration, but the interested reader may refer to [2] for such a survey.

In this paper, we introduce the main components of a new non-rigid registration technique which combines ideas from the feature-based and the intensity-based registration approaches. Given two images (2D or 3D), $I_s(\mathbf{x})$ and $I_t(\mathbf{x})$, of the same anatomical organs, taken from different patients or from the same patient over a period of time, our method performs matching between these two images in two main steps and outputs a spatial transformation $\mathbf{T}:\mathbb{R}^n \rightarrow \mathbb{R}^n$ ($n=$ 2, or 3), such that the similarity between the intensities $I_s(\mathbf{x})$ and $I_t(\mathbf{T(x)})$ is optimized. The first step of the introduced approach consists in globally aligning the two images. This corresponds to finding the optimal global transformation $T_{global}:\mathbf{x}\mapsto\mathbf{x}'$, which maps any point in one image into its corresponding point in the other image. In 3D space, the global motion can be modelled, for example, by a 12-parameter affine transformation which can be written as:

$$T_{global}(x,y,z)=\begin{pmatrix} a_{11} & a_{12} & a_{13} \\ a_{21} & a_{22} & a_{23} \\ a_{31} & a_{32} & a_{31} \end{pmatrix}\cdot\begin{pmatrix} x \\ y \\ z \end{pmatrix}+\begin{pmatrix} a_{14} \\ a_{24} \\ a_{34} \end{pmatrix}$$

In this work, the parameters of the T_{global} are determined through a minimization of the mean squared positional error between matched features. The scale space theory plays a major role here in extracting and matching these features. A novel approach to build robust and efficient 3D local invariant feature descriptors is introduced. The second step of the proposed approach is to find the optimal transformation, T_{local}, to model the local deformations of the imaged anatomy. The basic idea is to deform an object by evolving equi-spaced contours/surfaces in the target image to match those in the source image. These iso-surfaces are generated using fast marching level sets and the built local invariant feature descriptors are used as voxel signatures. Finally, we combine the local and the global transformations to produce our registration transformation $T(\mathbf{x})=T_{global}(\mathbf{x})+T_{local}(\mathbf{x})$. To validate our algorithm, we propose to simulate a 2D kidney deformation, and three physically plausible 3D brain deformation cases using the F.E. method. The registration accuracy with respect to (w.r.t.) the F.E. simulations is assessed by co-registering the deformed images with the original ones and comparing the recovered displacement fields with the biomechanically simulated ones. We compare the results of our technique to those obtained using our own implementation of the B-spline based free deformation approach [6]. This shows the potential of our method over the spline-based deformation technique.

II. METHOD

In this section, we describe the main steps of our deformable registration technique. The first task consists in building invariant feature descriptors which will be matched to find the correspondent pairs of control points.

A. Interest point detection

Interest points are usually selected in highly informative locations such as edges, corners, or textured regions. In the context of feature invariance, interest points should be selected so that they achieve the maximum possible repeatability under different imaging conditions.

The most challenging point is the invariance w.r.t. scale changes. Scale-space theory offers the main tools for selecting the most robust feature locations, or the interest points, against scale variations.

Authors are with the Computer Vision & Image Processing laboratory, University Of Louisville, Louisville, KY 40292, USA. Corresponding author (rachidf@cvip.uofl.edu)

In this work, the scale-space representation of an input 3D signal f is generated as follows. First, let's define $L_0 = g(\vec{x},t_0) * f(\vec{x})$ and $L_1 = g(\vec{x},t_1) * f(\vec{x})$, $t_1 = C.t_0$, where $C > 1$ is a real number, and $g(\vec{x},t) = \frac{1}{(2\pi t)^{\frac{3}{2}}} e^{\frac{-\vec{x}^T\vec{x}}{2t}}$. According to [17], the extrema (maxima and minima) of $\sigma^2\nabla^2 g$ produces the most stable image features. In other words, the locations of the extrema in the difference-of-Gaussian (DoG) hyper pyramid, i.e. scale-space levels, correspond to the most stable features with respect to scale changes.

Hence, the interest points are detected at the local extrema of the DoG hyper pyramid as described in [9].

B. Descriptor Building and Matching

We build our descriptor in 3D space using gradient orientations histograms with 2D polar-coordinate bins for neighboring cells which consist of voxels in the current level-neighborhood of every interest point. This method was previously used by us [9] for 2D medical applications and was proven to be efficient w.r.t. rotation and affine transformations in other applications as well [7]. The final descriptor is built as shown in Fig. 1. This vector is normalized to reduce the effect of linear intensity changes [7]. In this work, we use neighborhoods of 8x8x8 for both canonical gradient orientation and descriptor's entries, and cells of 4x4x4 which means that eight cells are used for building the entries of the descriptor. The descriptor is of size 8x8x4=256 and after adding the overhead of the original location, pyramid level, and the canonical orientation, the total descriptor size becomes $256+6=262$.

$$\frac{D(F_1,F_2)}{\min(D(F_1,F_2'))} < Threshold < 1, \text{ where } F_2' \neq F_1, \text{and } F_2' \neq F_2,$$

where, $D(\cdot,\cdot)$ is the Euclidean distance. Other distances may be used as well.

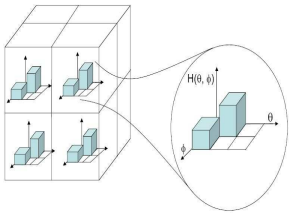

Fig. 1. The structure of the 3D feature descriptor. Only eight samples of neighboring cells and six histogram bins are shown in the figure for illustration purposes.

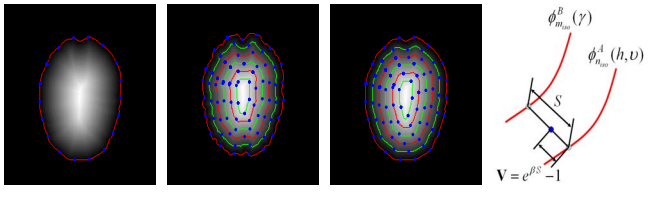

(a) (b) (c) (d)

Fig. 2. Cross sectional views of generated distance map & iso-surfaces before (a) and after (b,c) deformation. (d) The evolution scenario.

III. Global and Local Motion Modelling

To model the global motion between the two images, we build the 3D feature descriptor as described in Section II-B, and then we match the features of the reference image to those of the transformed image. The matched pairs are used to estimate a 3D global transformation through the gradient descent minimization of the mean squared positional error between the corresponding points. In this work, a 9 DOF affine transformation model is adopted.

To handle local deformations undergone by the imaged organ, we propose a new approach based on deforming the imaged organ over evolving closed and equi-spaced surfaces (iso-surfaces) to closely match the prototype. The evolution of the iso-surfaces is guided by an exponential speed function in the directions minimizing distances between corresponding pixel pairs on the iso-surfaces on both images. The proposed 3D local invariant feature descriptor (see Sec. II-B) is built for each point of each iso-surface after discretization. These descriptors, which are invariant to the image deformations, are used for image similarity measure.

The first step of our approach is to generate the distance map inside the brain images as shown in Fig. 2(a). The second step is to use this distance map to generate iso-surfaces as shown in Fig. 2(b),(c). Note that the number of iso-surfaces, which is not necessarily the same for both images, depends on the accuracy and the speed required by the user. The third step consists in finding the correspondences between the iso-surfaces. The final step is the evolution of the iso-surfaces; here, our goal is to deform the iso-surfaces in the first data set (target image) to match the iso-surfaces in the second data set (source image). Before stating the evolution equation, let us define the following:

- $\phi_n^A(\cdot,\nu)$ (resp. $\phi_m^B(\cdot)$) are the iso-surfaces on the target (resp. the source) image (A) (resp. (B)), with ν the iteration step,
- $S(h,\gamma_h)$ denotes the Euclidean distance between a iso-surface point h on image A and its corresponding iso-surface point γ_h on image B,
- $S^A_{n,n-1}(h)$ is the Euclidian distance between $\phi_n^A(h,\nu)$ and $\phi_{n-1}^A(h,\nu)$ at iteration ν,
- $V(\cdot)$ is the propagation speed function.

The propagation speed function V is selected so as to satisfy the following conditions: $V(h) = 0$ if $S(h,\gamma_h) = 0$, otherwise $V(h) \leq \min(S(h,\gamma_h), S^A_{n,n-1}(h), S^A_{n,n+1}(h))$. The latter condition, known as the smoothness constraint, prevents the current point from cross-passing the closest neighbor surfaces as shown in Fig. 2(d). Note that the function $V(h) = \exp(\beta(h)\cdot S(h,\gamma_h)) - 1$, satisfies the above conditions, where $\beta(h)$ is the propagation term such as, for each iso-surface point $h \in A$, $\beta(h) \preceq \frac{\ln[\min(S(h,\gamma_h), S^A_{n,n-1}(h), S^A_{n,n+1}(h))+1]}{S(h,\gamma_h)}$. Based on this speed function, the evolution process is governed by following equation:

$$\phi_n^A(h,\nu+1) = \frac{V(h)}{S(h,\gamma_h)}\phi_m^B(\gamma_h) + \frac{S(h,\gamma_h) - V(h)}{S(h,\gamma_h)}\phi_n^A(h,\nu),$$

where $h = 1, \ldots, \mathscr{H}$ denotes the iso-surface points on image A, and γ_h its corresponding iso-surface point on image B.

IV. Validation Approach using F.E.M.

In this section we propose to validate our deformable registration approach using the F.E.M.. Both 2D and 3D validation results are presented on some medical data.

A. 2D Case

Given a 2D image of the kidney, we simulate a deformation using a biomechanical model of the kidney tissue. The pair of images (deformed and non deformed ones) is used to test our algorithm. The Abaqus/CAE (Ver. 6.5) [14] environment was used to generate a cubic spline fit to the points representing the outer contour of the kidney object and then a 2D F.E. model was built from it. Fig. 3(a) and (b) show the 2D mesh before and after deformation, and the overlay of these two meshes, respectively. For the sake of generating a deformed shape only, we assumed the kidney tissue to be isotropic and homogeneous elastic material with a Young Modulus $E = 2500Pa$ and a Poisson Ratio $\nu = 0.4$. Note that this model does not reflect the results of any rheological experiments conducted on the kidney tissue. A uniformly distributed pressure $P = 100N$ was applied normal to the boundary of the kidney. The points on this boundary are allowed to move freely in the x and y directions, but are constrained to rotate around the z direction. The mesh consists of 1253 3-node linear plane stress angular elements. The average displacement of the induced deformation is $4.75mm$, the minimum is $1.19mm$, and the maximum is $6.9mm$. The accuracy of the registration method is assessed by registering the simulated deformed image to the original one and comparing the recovered point displacements with the bio-mechanically simulated ones. The average registration error is about $1.54mm$, with a maximum of $2.7458mm$, a minimum of $0.0221mm$, and a standard deviation of 0.5517. To illustrate these results, we present on Fig. 3, a set of ground truth locations (Abaqus simulated)(c), the corresponding recovered ones using our technique (d), and their overlay (e). The corresponding displacement field (see Fig. 3(f) shows the smoothness of the registration results. This proves the accuracy of the proposed non-rigid registration technique in 2D cases.

B. 3D Case

To validate the proposed registration technique in the 3D case, we use real brain MRIs. Two deformation types, characteristics for real patient-specific acquisitions, are simulated: gravity-induced deformation and ventricles contraction. For the first type of deformations, two biomechanical models for

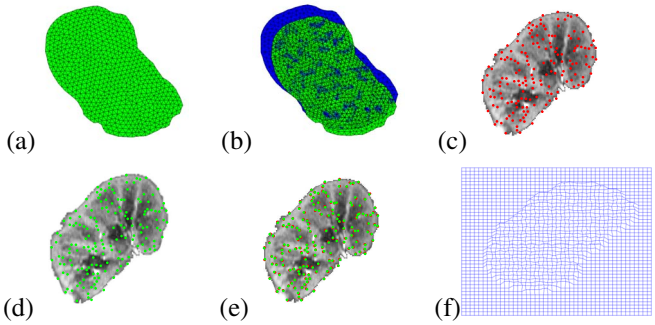

Fig. 3. Validation of our non-rigid registration technique in 2D case

the brain tissues are used separately: the linear elastic model (case 1) and the hyperelastic model (case 2). The latter model is also chosen for the ventricle contraction case (case 3).

*a) **Model Construction**:* For the construction of the brain F.E. models for the three cases, the same T1-weighted MRIs of a normal brain of size $256x256x198$ and a voxel size of $1x1x1mm^3$ is used as input data. Firstly, the brain volume is skull-stripped (i.e., non brain tissue removed) and segmented into white matter (W.M.), gray matter (G.M.), and CSF ventricles, using the FSL package [13]. Secondly, the segmented images are input into the TetSplit [4] program to generate 3D linear tetrahedral meshes. The material properties for different tissue types were carefully chosen from the literature [3], [10], [11]. As boundary conditions (B.C.),

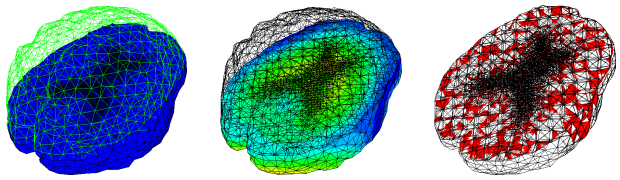

Fig. 4. From left to right: 3D F.E. Mesh, Deformed Mesh, and Z-plane cut of overlayed meshes before (red) and after (white) deformation.

we fixed the points of the brain where the falx meets the skull and we considered the falx to have the same material parameters as those assigned to the brain. The remaining points on the brain outer surface were allowed to slide freely in the direction tangent to the brain surface only. Finally, to anticipate the contact between the ventricle walls during the simulations, we modelled the ventricles as a hyperfoam material using the Ogden model (see Abaqus Doc.) with material parameters as in [3]. An example of simulated deformation (case 2) is shown in Fig. 4.

*b) **Generation of Gray-Scale Deformed Images**:* To be used in the registration process, the original images are deformed using the dense displacement field obtained from

each simulation. Within the F.E. framework, the displacement $\vec{u}$ of any voxel $\vec{x}$ lying within an element *el* in the model, is defined as a weighted interpolation of the node displacements $\vec{u}_j^{el}$ as: $\vec{u}(\vec{x}) = \sum_{j=1}^{4} h_j^{el}(\vec{x})\vec{u}_j^{el}$, where $h_j^{el}(.)$, $j = 1, \cdots, 4$, are the element shape functions [12]. Using this interpolator to generate deformed images overcomes the problem of residual errors at the F.E. node locations that may appear when using, for example, B-spline based interpolation [15].

*c) **Validation Results**:* For each one of the simulated deformation cases, we have run both our approach and our own implementation of the FFD technique. This implementation is based on maximizing the mutual information w.r.t. the 12 parameters of the affine transformation as well as to the control point displacements using a genetic algorithm. The optimal size of the control point lattice was determined also through this optimization step. The accuracy of our technique has been quantitatively assessed at the F.E. node positions by comparing the recovered voxel displacements with the simulated ones. Table I summarizes the error statistics for the 3 cases using the two registration techniques. One can see that our algorithm outperforms the other one in all of the 3 cases, with an average accuracy almost five times higher. Moreover, our algorithm executes faster than the other method for all the considered cases with an average speed 3 to 4 times higher. Both algorithms were implemented using Matlab, and were run on the same PIII-PC.

TABLE I

QUANTITATIVE ASSESSMENT OF THE REGISTRATION ACCURACY. COMPARISON WITH OUR OWN IMPLEMENTATION OF THE FREE-FORM DEFORMATION (OWN_FFD) METHOD. DISPLACEMENTS CORRESPOND TO THE SIMULATED ONES. ALL UNITS ARE IN (**MM**).

		Case 1	Case 2	Case 3
Max. Displacement		9.88	4.76	1.68
Mean Displacement $\pm$ std. dev.		6.08 ± 1.06	2.25 ± 0.68	0.55 ± 0.38
Max Error	Ours	2.08	2.36	0.63
	Own_FFD	9.18	7.46	4.03
Mean Error $\pm$ std. dev.	Ours	1.20 ± 1.58	1.32 ± 0.38	0.36 ± 0.31
	Own_FFD	5.15 ± 1.50	4.20 ± 1.26	2.29 ± 0.67

V. CONCLUSION

In this paper, we presented a novel approach for 3D non-rigid registration. The proposed approach uses fast marching level sets method to generate iso-surfaces. These iso-surfaces are evolved to handle the local deformations. A new approach was introduced to build 3D local invariant feature descriptors using scale-space theory. These descriptors are used both in the estimation of the global transformation parameters, and in the evolution process of the iso-surfaces. The use of these descriptors provides a robust matching under different geometrical and intensity variations, which enhances the registration accuracy. The evaluation results show the high accuracy of the proposed approach over free form deformation approaches. The performance of our algorithm was validated using the F.E. method. Both 2D and 3D deformation cases were simulated for quantitative assessment of the registration accuracy. In all of these cases, our method was faster and more accurate than our independent implementation of the FFD method. In the future, we will test our method on other image modalities, and we will compare it to other techniques, such as HAMMER [5]. A sensitivity to noise analysis will also be conducted in future works.

REFERENCES

[1] D. Shen and C. Davatzikos, "Hammer: Heirarchical attribute matching mechanism for elastic registration", *IEEE Trans. Med. Imaging* Vol. 21(11), 2002, pp. 1421-1439

[2] B. Zitova and J. Flusser, "Image registration methods: a survey", *Image and Vision Computing*, vol. 21, 2003, pp 977-1000.

[3] K. Miller and K. Chinzei, "Mechanical properties of brain tissue in tension", *J. Of Biomechanics*, vol. 35, 2002, pp 483-490.

[4] A. Mohamed and C. Davatzikos, "Finite element mesh generation and remeshing from segmented medical images", *ISBI2004, From Nano to Macro, Arlington, VA*, 2004.

[5] D. Shen and C. Davatzikos, "HAMMER: Hierarchical Attribute Matching Mechanism for Elastic Registration", *IEEE Transaction on Medical Imaging*, vol. 21 (11), 2002, pp 1421-1439.

[6] D. Rueckert, L.I.Sonoda, C. Hayes, D.L.G. Hill, M.O. Leach, and D.J. Hawkes, "Nonrigid registration using free-form deformations: Application to breast mr images", *IEEE Transactions on Medical Imaging*, vol. 18(8), 1999, pp 712-721.

[7] D.G. Lowe, "Distinctive image features from scale-invariant keypoints", *Int. J. Comput. Vision*, vol. 60(2), 2004, pp 91-110.

[8] T. Lindeberg, "Scale-Space Theory in Computer Vision", *Kluwer Academic Publishers, Norwell, MA, USA*, 1994.

[9] Author's work

[10] M. I. Miga, D. W. Roberts, F.E. Kennedy, L. A. Platenik, A. Hartov, K. E. Lunn, and K. D. Paulsen, "Modeling of Retraction and Resection for Intraoperative Updating of Images", *Neurosurgery*, vol. 49(1), 2001, pp. 75-85.

[11] O. Clatz, H. Delingette, I. F. Talos, A. J. Golby, R. Kikinis, F. A. Jolesz, N. Ayache, and S. K. Warfield, "Robust Non-Rigid Registration to Capture Brain Shift form Intra-Operative MRI", *MICCAI'05*, pp. 295-302.

[12] O. C. Zienkiewicz and R. L. Taylor, "The Finite Element Method", *ButterWorth-Heimann*, vol. Vol II, 2000.

[13] http://www.fmrib.ox.ac.uk/fsl/

[14] http://www.abaqus.com

[15] J. A. Schnabel et al., "Validation of Non-Rigid Image Registration Using Finite-Element Methods: Application to Breast MR Images", IEEE-TMI, vol. 22 (2), 2003, pp. 238-247.

[16] M. I. Miga et al., "Model-updated image-guided neurosurgery using finite element method: Incorporation of the falx cerebri", MICCAI99.

[17] K. Mikolajczyk and C. Schmid, "An Affine Invariant Interest Point Detector", *Proceedings of the 7th European Conference on Computer Vision-Part I (ECCV '02)*, 2002, ISBN 3-540-43745-2, pp. 128-142, Springer-Verlag, Copenhagen, Denmark.